

Anharmonicity of multi-octupole-phonon excitations in ^{208}Pb : analysis with multi-reference covariant density functional theory and subbarrier fusion of $^{16}\text{O}+^{208}\text{Pb}$

J. M. Yao^{1,2,3} and K. Hagino^{2,4,5}

¹*School of Physical Science and Technology, Southwest University, 400715 Chongqing, China*

²*Department of Physics, Tohoku University, Sendai 980-8578, Japan*

³*Department of Physics and Astronomy, University of North Carolina, Chapel Hill, NC 27516-3255, USA*

⁴*Research Center for Electron Photon Science, Tohoku University, 1-2-1 Mikamine, Sendai 982-0826, Japan*

⁵*National Astronomical Observatory of Japan, 2-21-1 Osawa, Mitaka, Tokyo 181-8588, Japan*

We discuss anharmonicity of the multi-octupole-phonon states in ^{208}Pb based on a covariant density functional theory, by fully taking into account the interplay between the quadrupole and the octupole degrees of freedom. Our results indicate the existence of a large anharmonicity in the transition strengths, even though the excitation energies are similar to those in the harmonic limit. We also show that the quadrupole-shape fluctuation significantly enhances the fragmentation of the two-octupole-phonon states in ^{208}Pb . Using those transition strengths as inputs to coupled-channels calculations, we then discuss the fusion reaction of $^{16}\text{O}+^{208}\text{Pb}$ at energies around the Coulomb barrier. We show that the anharmonicity of the octupole vibrational excitation considerably improves previous coupled-channels calculations in the harmonic oscillator limit, significantly reducing the height of the main peak in the fusion barrier distribution.

PACS numbers: 21.60.Jz, 23.20.-g, 21.10.Re, 25.70.Jj

Collective vibrational excitations exist commonly in many-fermion systems [1]. Here, the concept of *phonon* is an important keystone to understand these excitations. For instance, for finite nuclear systems, vibrations of the nuclear surface are treated as elementary excitations [2, 3]. The phonons for these vibrations are boson-like in character and multiple excitations of the same type are possible, resulting in *multi-phonon* states [2]. In a harmonic vibration, all the levels in a phonon multiplet are degenerate in energy and the energy spacing between neighboring multiplets is a constant. The energy patterns close to such harmonic vibration have been observed in nearly spherical nuclei in different mass regions, and these states have been primarily interpreted as multipole phonon states [2, 4, 5].

From a microscopic viewpoint, however, the collective excitations are generated by a coherent superposition of quasiparticle excitations of fermions in orbits close to the Fermi surface. The Pauli principle correction, together with residual interactions among phonons (that is, mode-mode couplings), modifies the structure of multi-phonon states and make them highly fragmented [6]. To assess the degree of such anharmonicity is a fundamental question in nuclear physics, that needs to be studied more extensively. In particular, we mention that recent studies on the anharmonicity in the multi-quadrupole-phonon states have questioned the concept of low-energy vibrational modes in atomic nuclei [7, 8].

The double-magic nucleus ^{208}Pb provides an ideal laboratory to examine the concept of *multi-octupole-phonon* excitations in nuclear systems, as the first excited 3^- state of this nucleus has long been interpreted as a collective one-octupole-phonon state [9]. In the past decades, several experimental searches for the *two-*

octupole-phonon (TOP) states in ^{208}Pb have been carried out [10–13]. Even though many of the TOP members have been identified, the multi-phonon excitations in ^{208}Pb have not yet been understood completely. This is the case especially for the nature of the TOP multiplets, which has been predicted to show a strong fragmentation [13–15].

Incidentally, heavy-ion fusion reactions provide an alternative way to probe the multi-phonon excitations in atomic nuclei, which significantly affect the subbarrier fusion cross sections [16–19] as illustrated by coupled-channels calculations [16, 20, 21]. Previous coupled-channels calculations for the fusion reaction of $^{16}\text{O}+^{208}\text{Pb}$ based on multi-harmonic-phonon excitations fail to reproduce the observed energy dependence of fusion cross sections [22–24], and overestimate the height of the main peak in the so called fusion barrier distribution [25]. It has been a long-standing unsolved question how the fusion cross sections for the $^{16}\text{O}+^{208}\text{Pb}$ system can be accounted for by the coupled-channels approach.

In this paper, we for the first time examine the concept of multi-octupole-phonon excitations in ^{208}Pb in the microscopic framework of generator coordinate method (GCM) based on a covariant energy density functional [26]. This beyond mean-field approach is also referred to as multi-reference covariant density functional theory and has been rapidly developed in the past decade [27–29]. In this method, collective vibrational excitations are described as fluctuations in nuclear shapes in a full microscopic manner and therefore the Pauli principle correction to the phonon excitations is taken into account automatically. We show that this method is capable to capture the main characters of nuclear multipole phonon excitations, which are generally

fragmented by its internal fermionic structure and by coupling to other shape degrees of freedom. We show that these anharmonic features considerably improve the coupled-channels calculations for the fusion reaction of $^{16}\text{O}+^{208}\text{Pb}$, significantly reducing the height of the main peak in the fusion barrier distribution.

In the multi-reference covariant density functional theory, the wave functions for nuclear collective states are constructed by superposing a set of quantum-number projected nonorthogonal mean-field reference states $|\beta_2\beta_3\rangle$ around the equilibrium shape. Here, the reference states $|\beta_2\beta_3\rangle$ are obtained by deformation constrained relativistic mean-field calculations with the quadrupole and octupole deformation parameters, β_2 and β_3 , respectively. The wave functions thus read

$$|JM\pi\rangle = \sum_q f^{J\pi}(q) \hat{P}_{M0}^J \hat{P}^N \hat{P}^Z \hat{P}^\pi |q\rangle, \quad (1)$$

where q refers to (β_2, β_3) and \hat{P} 's are projection operators onto the angular momentum J , the parity ($\pi = \pm$), and the neutron and proton numbers (N, Z) [3]. For the sake of simplicity, we have restricted all the reference states $|q\rangle$ to be axially deformed. We note that the effects of pairing vibrations are not taken into account in the present calculation, even though they may have an influence on low-lying excited 0^+ states [30]. The weight function $f^{J\pi}(q)$ in Eq. (1) as well as the energy E_J^π for each GCM state $|JM\pi\rangle$ are determined by the Hill-Wheeler-Griffin equation [31]. As in our previous studies [27], the mixed-density prescription is adopted for the energy overlap in the Hamiltonian kernel. In the calculations presented below, we employ the relativistic energy functional PC-F1 [32]. The pairing correlation among the nucleons is treated in the BCS approximation with a density-independent δ -force supplemented with a smooth energy cutoff [33]. The strength parameters in the pairing force are chosen according to the PC-F1 force [32].

We first examine the concept of one-dimensional vibration in ^{208}Pb with octupole degree of freedom, by freezing the quadrupole degree of freedom at $\beta_2 = 0$. The deformation energy curve in the mean-field approximation as well as the projected energy curve for $J^\pi = 0^+$ are shown in Fig. 1. The excitation energies of natural-parity ‘‘phonon’’ states and the collective wave functions defined by $g^{J\pi}(q) \equiv \sum_{q'} [\mathcal{N}_{q,q'}^{J\pi}]^{1/2} f^{J\pi}(q')$ for the 0_1^+ , 3_1^- , $[3^- \otimes 3^-]_{6^+}$, and $[3^- \otimes 3^- \otimes 3^-]_{9^-}$ states are also shown, where $\mathcal{N}_{q,q'}^{J\pi}$ is the norm kernel in the Hill-Wheeler-Griffin equation [28]. The mean-field energy curve is almost parabolic and is centered at $\beta_3 = 0$. As expected, the dynamical octupole effect originated from the symmetry restoration generates two octupole minima and shifts the dominant component in the 0^+ state to an octupole-deformed configuration with $|\beta_3| \sim 0.1$. One can also see that the multiples of two- and three-‘‘phonon’’ states appear at similar excitation energies to each other. The

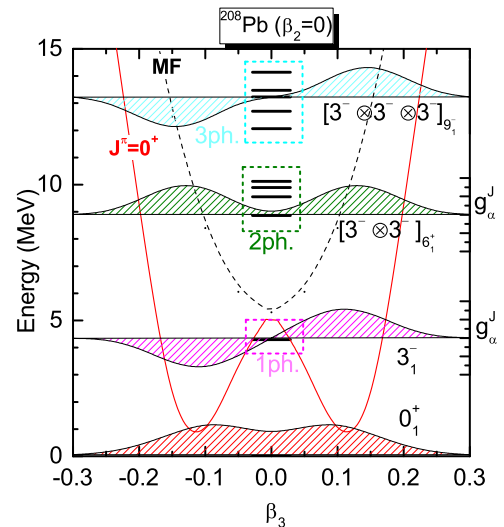


FIG. 1: (Color online) The total energy (normalized to the GCM ground state) of the ^{208}Pb nucleus as a function of octupole deformation parameter β_3 . The quadrupole degree of freedom is frozen at $\beta_2 = 0$. The energy curve with projection onto the particle numbers (N, Z) and the spin-parity of 0^+ is also shown by the solid line, together with the excitation energies and the collective wave functions for the states.

spin-average of the excitation energies for the natural-parity two- and three-octupole phonon states is 9.6 MeV and 13.1 MeV, respectively, which is about twice and three times the energy of the one-octupole phonon state, 4.3 MeV, close to ~ 4.0 MeV from non-relativistic GCM calculations [34, 35] (the excitation energies are expected to be lowered down if the cranking mean-field states are adopted in the configuration mixing calculations [36, 37]). Notice, however, that there are some energy displacements, indicating the existence of anharmonicity. The energy displacement appears to increase with the number of the ‘‘phonons’’ in the states. As can be seen in the figure, the wave functions for the 0_1^+ and 3_1^- states show a similarity to the wave functions for the zero and one-phonon states of a harmonic oscillator, while those of the $[3^- \otimes 3^-]_{6^+}$ and $[3^- \otimes 3^- \otimes 3^-]_{9^-}$ states are considerably distorted.

It is interesting to notice that an anharmonicity is stronger in the transition strengths as shown in Fig. 2(c), where the $E3$ transition strength from the 3_1^- state to the ground state is underestimated by a factor of more than two. Moreover, the $E2$ transition strength from the first 2^+ state to the ground state is underestimated by three orders of magnitude. The strength of the $E3$ transition from the two-phonon multiplets to the 3_1^- state is also much larger than twice the $B(E3)$ value from the 3_1^- state to the ground state. In particular, the $E3$ transition from the $[3_1^- \otimes 3_1^-]_{0^+}$ state to the 3_1^- state is much stronger than that from the other multiplets of the TOP states. We note that a large anharmonicity in the

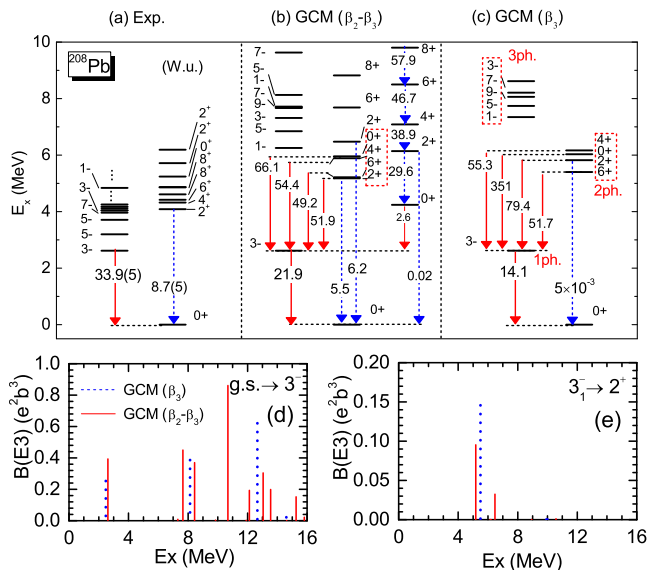


FIG. 2: (Color online) The low-lying energy spectra of ^{208}Pb obtained by mixing the octupole-quadrupole ($\beta_3 - \beta_2$) deformed configurations (the panel (b)) and by mixing only the octupole (β_3) deformed configurations (the panel (c)), in comparison with the experimental data taken from Ref. [38] (the panel (a)). The panels (d) and (e) show the $E3$ transition strengths from the the ground state to 3^- states and from the first 3^- state to 2^+ states, respectively, as a function of the excitation energy of the final states. In the panels (a)-(c), the red solid and the blue dashed lines indicate the $E3$ and $E2$ transition strengths (in W.u.), respectively. All the calculated excitation energies are scaled to the empirical excitation energy of the lowest 3^- state by dividing them by a constant factor.

transition strengths has been found also in the “multi-quadrupole-phonon” excitations in Refs. [7, 8].

To examine the anharmonicity arising from the coupling between the octupole and the quadrupole shape fluctuations, we next carry out the GCM calculation in the two-dimensional (β_2, β_3) deformation plane. The calculated low-lying energy spectra are shown in Fig. 2(b), where only natural-parity states are plotted. Here, the spectra are scaled by a constant factor so that the energy of the first 3^- state matches with the empirical value, 2.62 MeV. Notice that the inclusion of the quadrupole shape fluctuation slightly alters the excitation energies of the $[3_1^- \otimes 3_1^-]_{0^+, 2^+, 4^+, 6^+}$ states. One can see that, after including this effect, the transition strengths for the $3_1^- \rightarrow 0_1^+$ and the $2_1^+ \rightarrow 0_1^+$ transitions are closer to the experimental data. The $B(E3; 3_1^- \rightarrow 0_1^+)$ value is consistent with 21.93 W.u. by the Gogny D1S force [35], although it is slightly larger than 18.7 W.u by the Skyrme SLy4 force [34]. Moreover, the electric dipole transition strengths are also well reproduced by this calculation. For instance, we obtain the $B(E1)$ value from the first 4^+ state to the first 5^- state to be 1.5×10^{-4} W.u.,

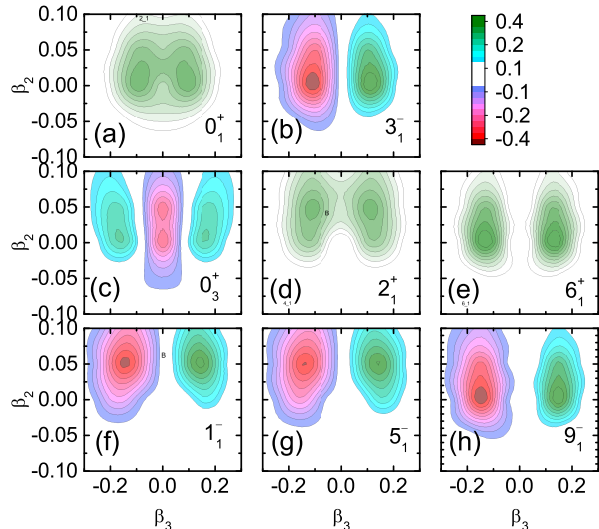


FIG. 3: (Color online) The distribution of the collective wave functions $g^{J\pi}$ for several selected low-lying states of ^{208}Pb shown in Fig. 2(b).

which is compared to the experimental upper bound of 1.0×10^{-4} W.u. [11]. We note that, in the octupole-quadrupole shape-mixing calculation, the $E3$ transition strengths from the four TOP states to the 3_1^- state are similar to each other, about three times the $B(E3)$ value from the 3_1^- state to the ground state. Figures 2(d) and (e) show the calculated $B(E3)$ values from the ground state to 3^- state and those from the first 3^- state to 2^+ states as a function of the excitation energy of the final states, respectively. The solid and the dotted lines indicate the results of the octupole-quadrupole shape fluctuation and of the octupole vibration only, respectively. One can see that generally the $E3$ transitions become more fragmented after taking into account the fluctuation in the quadrupole shape. In particular, the $E3$ transition from the 3_1^- state to excited 2^+ states are strongly quenched. Similar phenomenon is also found in the $E3$ transitions from the 3_1^- state to other excited states (not shown here).

Figure 3 shows the distribution of the collective wave functions for the ground state and some selected excitation states. Comparing with the wave functions in Fig. 1, one can see a rather large fluctuation along the quadrupole deformation in all the states. For the multiplets of the TOP states, only the 0^+ state has two nodes along β_3 direction, showing again the anharmonicity in the wave functions.

We have repeated the GCM calculation using the PC-PK1 force [39]. The calculated excitation energies and electric multipole transition strengths for the one- and two-octupolephonon states turned out to be similar to those by the PC-F1 force. However, we have found

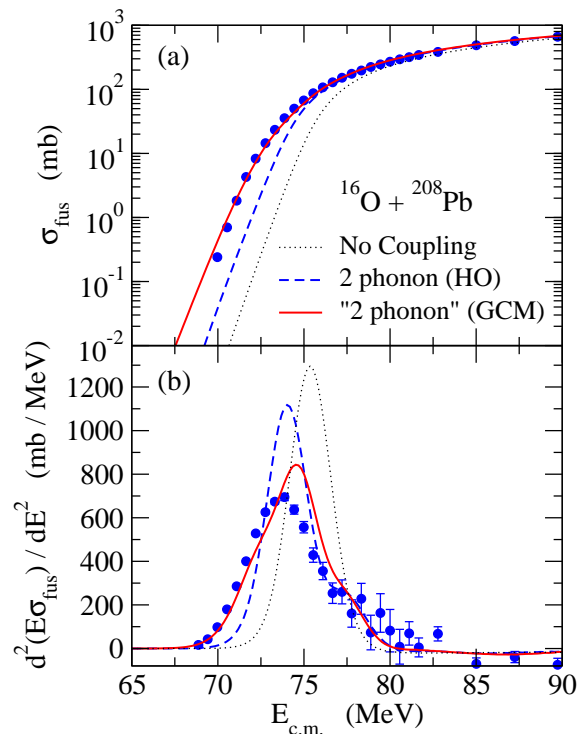


FIG. 4: (Color online) The fusion cross sections (upper panel) and the fusion barrier distributions (lower panel) for the $^{16}\text{O}+^{208}\text{Pb}$ system obtained with the semi-microscopic coupled-channels calculation with the coupling strengths from the MR-DFT calculations (the solid line). The dashed and the dotted lines show the results of the two-phonon coupling in the harmonic oscillator limit and of the no-coupling limit, respectively. The experimental data are taken from Ref. [22].

that the 2^+ states and high-lying states with the PC-PK1 force may have a problem of convergence, as they are much more sensitive to the model space than those by the PC-F1 force, even though both PC-F1 and PC-PK1 forces give much better convergent solutions for the quadrupole-phonon states in $^{58,60}\text{Ni}$ [40]. In view of this, we present only the PC-F1 results in this paper.

In order to further test the results of the present calculation for the ^{208}Pb nucleus, we next discuss the sub-barrier fusion reaction of the $^{16}\text{O}+^{208}\text{Pb}$ system. To this end, we employ the semi-microscopic approach [40] and solve the coupled-channels equations by using the transition strengths from the GCM calculations as inputs. In this approach, the internuclear potential and the coupling potentials are generated from a phenomenological deformed Woods-Saxon potential. For this, we use the parameters of $V_0=178$ MeV, $R_0=0.978 \times (16^{1/3} + 208^{1/3})$ fm, and $a=1.005$ fm, which are similar to those used in Ref. [22]. In the coupled-channels calculations, in addition to the entrance channel, we include the one-octupole phonon state, 3_1^- , at 2.615 MeV, the ‘‘one-quadrupole’’ phonon state, 2_1^+ , and several states which are strongly coupled to those 3_1^- and 2_1^+ states by the octupole and

the quadrupole couplings. The whole TOP candidate states are included in this model space. As is shown in Ref. [40], we scale all the excitation energies to the empirical excitation energy of the 3_1^- state. We also scale all the coupling strengths to the empirical coupling strength between the ground state and the 3_1^- state, that is, $\beta = 0.144$, which is estimated from the measured $B(E3)$ strength with the radius parameter of $r_0=1.1$ fm. The resultant coupled-channels equations are solved using the computer code CCFULL [41].

The solid line in Fig. 4 is the fusion cross sections (the upper panel) and the fusion barrier distribution (the lower panel) so obtained. Here, the fusion barrier distribution is defined as the second energy derivative of the product of the energy E and fusion cross section σ_{fus} , that is, $d^2(E\sigma_{\text{fus}})/dE^2$ [17, 25]. This is compared to the two-phonon calculations in the harmonic oscillator limit (the dashed line) and to the single-channel calculation (the dotted line). For the former, we include the 3_1^- , 2_1^+ , $(3_1^-)^2$, $(2_1^+)^2$, and $3_1^- \otimes 2_1^+$ states within the harmonic oscillator coupling scheme [16]. It has been a long-standing problem that for this particular system the coupled-channels calculation with the harmonic oscillator couplings overestimates the height of the main peak in the barrier distribution [22–24]. It is remarkable that the present GCM calculation yields a much lower peak in the fusion barrier distribution, leading to a much better agreement with the experimental data both for the fusion cross sections and for the barrier distribution. For this good reproduction, it turns out that the coupling between the 3_1^- and the 2_1^+ states, as well as the couplings between the TOP states and the excited negative parity states, play an important role. In the previous coupled-channels calculations, the 3^- , 2_1^+ and the 5_1^- states have been treated as independent phonon states, and these couplings were absent in the calculations. In contrast, in the present GCM calculation, the 2_1^+ and the 5_1^- states have in part the two and three octupole phonon characters, respectively. Likewise, the 1^- states have both the $(3_1^-)^3$ and the $3_1^- \otimes 2_1^+$ characters. Apparently those anharmonicity effects in the transition strengths lead to the strong couplings between the ground state and those states via multiple octupole excitations, significantly improving the previous coupled-channels calculations.

In summary, the multi-octupole-phonon excitations in ^{208}Pb have been examined with the multi-dimensional GCM calculations based on a covariant energy density functional. We have shown that the coupling to quadrupole shape fluctuation leads to a stronger fragmentation of the double-octupole phonon states and also enhances the $E3$ transition strength between the ground state and the single-octupole phonon state. These calculated transition strengths have then been used as inputs to the coupled-channels equations in order to discuss the sub-barrier fusion reaction of $^{16}\text{O}+^{208}\text{Pb}$. We have shown that these anharmonicity effects in the transition

strengths play an important role in this reaction, leading to a much better reproduction of fusion barrier distribution as compared to the previous coupled-channels calculations.

Our calculations indicate that anharmonicity of nuclear vibrations is much larger in the collective wave functions and in the transition properties as compared to the anharmonicity in the excitation energies. An interesting feature is that the anharmonicity may be large even if the energy spectrum resembles a harmonic oscillator. It will be interesting to reexamine systematically nuclear vibrations with a fully microscopic theory such as the multi-reference density functional approaches based on both nonrelativistic and relativistic energy functionals in future.

We thank D. J. Hinde and T. Ichikawa for useful discussions. This work was partially supported by the NSFC under Grant Nos. 11575148, 11475140, and 11305134, and JSPS KAKENHI Grant Number 2640263.

-
- [1] G. F. Bertsch and R. A. Broglia, *Oscillations in Finite Quantum System* (Cambridge University Press, Cambridge, 1994).
- [2] A. Bohr and B. Mottelson, *Nuclear Structure* (Benjamin, New York, 1975), Vol. 2.
- [3] P. Ring and P. Schuck, *The Nuclear Many-Body Problem* (Springer-Verlag, Berlin, 1980).
- [4] T. Aumann, P. F. Bortignon, and H. Emling, Nucl. Part. Sci. **48**, 351 (1998).
- [5] F. Corminboeuf, T. B. Brown, L. Genilloud, C. D. Hannant, J. Jolie, J. Kern, N. Warr, and S. W. Yates, Phys. Rev. Lett. **84**, 4060 (2000).
- [6] D. M. Brink, A. F. R. de Toledo Piza, and A.K. Kerman, Phys. Lett. **19B**, 413 (1965).
- [7] P. E. Garrett, K. L. Green, and J. L. Wood, Phys. Rev. **C78**, 044307 (2008); P. E. Garrett and J. L. Wood, J. Phys. **G37**, 064028 (2010).
- [8] E. A. Coello Perez and T. Papenbrock, Phys. Rev. **C92**, 064309 (2015).
- [9] I. Hamamoto, Phys. Rep. **10**, 63 (1974).
- [10] M. Yeh, P. E. Garrett, C. A. McGrath, S. W. Yates, and T. Belgia, Phys. Rev. Lett. **76**, 1208 (1996).
- [11] M. Yeh, M. Kadi, P. E. Garrett, C. A. McGrath, S. W. Yates, and T. Belgia, Phys. Rev. **C57**, R2085 (1998).
- [12] K. Vetter, A. O. Macchiavelli, D. Cline, H. Amro, S. J. Asztalos, B. C. Busse, R. M. Clark, M. A. Deleplanque, R. M. Diamond, P. Fallon, R. Gray, R. V. F. Janssens, R. Krücken, I. Y. Lee, R. W. MacLeod, E. F. Moore, G. J. Schmid, M. W. Simon, F. S. Stephens, and C. Y. Wu, Phys. Rev. **C58**, R2631 (1998).
- [13] B. D. Valnion, V. Yu. Ponomarev, Y. Eisermann, A. Gollwitzer, R. Hertenberger, A. Metz, P. Schiemenz, and G. Graw, Phys. Rev. **C63**, 024318 (2001).
- [14] V. Yu. Ponomarev and P. von Neumann-Cosel, Phys. Rev. Lett. **82**, 501 (1999).
- [15] B. A. Brown, Phys. Rev. Lett. **85**, 5300 (2000).
- [16] K. Hagino and N. Takigawa, Prog. Theor. Phys. **128**, 1001 (2012).
- [17] M. Dasgupta, D.J. Hinde, N. Rowley, and A. M. Stefanini, Annu. Rev. Nucl. Part. Sci. **48**, 401 (1998).
- [18] A. B. Balantekin and N. Takigawa, Rev. Mod. Phys. **70**, 77 (1998).
- [19] B. B. Back, H. Esbensen, C. L. Jiang, and K. E. Rehm, Rev. Mod. Phys. **86**, 317 (2014).
- [20] K. Hagino, N. Takigawa, and S. Kuyucak, Phys. Rev. Lett. **79**, 2943 (1997).
- [21] K. Hagino, S. Kuyucak, and N. Takigawa, Phys. Rev. C **57**, 1349 (1998).
- [22] C. R. Morton, A. C. Berriman, M. Dasgupta, D. J. Hinde, J. O. Newton, K. Hagino, and I. J. Thompson, Phys. Rev. **C60**, 044608 (1999).
- [23] H. Esbensen and S. Misicu, Phys. Rev. C **76**, 054609 (2007).
- [24] S. Yusa, K. Hagino, and N. Rowley, Phys. Rev. **C85**, 054601 (2012).
- [25] N. Rowley, G.R. Satchler, and P.H. Stelson, Phys. Lett. **B254**, 25 (1991).
- [26] T. Niksic, D. Vretenar, P. Ring, Prog. Part. Nucl. Phys. **66**, 519 (2011).
- [27] J. M. Yao, J. Meng, P. Ring, and D. Vretenar, Phys. Rev. C **81**, 044311 (2010); J. M. Yao, K. Hagino, Z. P. Li, J. Meng, and P. Ring, Phys. Rev. C **89**, 054306 (2014).
- [28] J. M. Yao, E. F. Zhou, and Z. P. Li, Phys. Rev. **C92**, 041304(R) (2015).
- [29] E. F. Zhou, J. M. Yao, Z. P. Li, J. Meng, and P. Ring, Phys. Lett. **B753**, 227 (2016).
- [30] P. F. Bortignon, in *Elementary Modes of Excitation in Nuclei*, Proceedings of the International School of Physics “Enrico Fermi”, Course LXIX, Varenna, 1976, edited by A. Bohr and R.A. Broglia (North Holland, Amsterdam, 1977).
- [31] D. L. Hill and J. A. Wheeler, Phys. Rev. **89**, 1102 (1953); J. J. Griffin and J. A. Wheeler, *ibid.* **108**, 311 (1957).
- [32] T. Bürvenich, D. G. Madland, J. A. Maruhn, and P.-G. Reinhard, Phys. Rev. C **65**, 044308 (2002).
- [33] S. J. Krieger, P. Bonche, H. Flocard, P. Quentin, and M. S. Weiss, Nucl. Phys. **A 517**, 275 (1990).
- [34] P.-H. Heenen, A. Valor, M. Bender, P. Bonche, and H. Flocard, Eur. Phys. J. **A11**, 393 (2001).
- [35] L. M. Robledo, EPJ Web of Conferences **66**, 02091 (2014).
- [36] Z. P. Li, T. Niksic, P. Ring, D. Vretenar, J. M. Yao, and J. Meng, Phys. Rev. **C86**, 034334 (2012).
- [37] M. Borrajo, T. Rodriguez and J. L. Egidio, Phys. Lett. **B746**, 341-346 (2016).
- [38] National Nuclear Data Center, <http://www.nndc.bnl.gov/>.
- [39] P. W. Zhao, Z.P. Li, J.M. Yao, and J. Meng, Phys. Rev. **C82**, 054319 (2010).
- [40] K. Hagino and J. M. Yao, Phys. Rev. **C91**, 064606 (2015).
- [41] K. Hagino, N. Rowley, and A. T. Kruppa, Comp. Phys. Comm. **123**, 143 (1999).